[Steps For Civil, Constructions and Environmental Engineering (SCCEE)](#)
ISSN: 3005-8198 (online) / 3005-818X (print)
Volume 4, Issue 2 (April – June 2026), pp: 14-24

Review Article

Interface-Controlled Shear Behavior of Masonry: Insights from a Database of Triplet Tests

Yousra Ouled Abdelkader [1,a*], George Wardeh [1,b], Hanaa Fares [1,c], Firas Al-Mahmoud [2,d]

[1] L2MGC, CY Cergy-Paris University, 5 mail Gay Lussac, 95031 Neuville-sur-Oise, France.
[2] University of Lorraine, CNRS, IJL, Nancy F-54000, France.

E-mail: yousra.ouled-abdelkader@cyu.fr [a,*], george.wardeh@cyu.fr [b], hanaa.fares@cyu.fr [c], firas.al-mahmoud@univ-lorraine.fr [d]

Received: 17 November 2025 | Revised: 24 February 2026 | Accepted: 06 April 2026 | Published: 22 May 2026

Abstract

The shear behavior of masonry bed joints governs the structural response of masonry assemblies under lateral loading yet remains difficult to predict due to material heterogeneity and interface-controlled mechanisms. Despite the prevalence of triplet shear tests in characterizing joint behavior, existing models frequently employ oversimplified assumptions, most notably a single linear Mohr–Coulomb failure envelope calibrated from limited parameters. This study addresses these limitations through a comprehensive, data-driven analysis of masonry shear behavior based on a harmonized literature database. A total of 183 masonry triplet shear tests were collected from published studies. The dataset under consideration is extensive, encompassing a broad array of masonry units, mortar types, mixture proportions, and interface conditions. A series of statistical correlation analyses were conducted to ascertain the relationships between brick-and-mortar compressive strengths, mortar composition, and the shear parameters of cohesion and friction. The analysis was restricted to monotonic loading conditions. The findings indicate that compressive strength parameters demonstrate a weak or negligible correlation with shear properties. Conversely, the composition of mortar, particularly the proportion of sand to binder, exerts a predominant influence on friction control. Furthermore, the findings indicated that cohesion and friction exhibited significant independence, thereby underscoring the multifaceted mechanisms underlying masonry shear resistance. The regression and nearest neighbor predictive approaches were validated against independent experimental datasets covering weak to strong masonry systems, successfully reproducing observed trends and behavioral hierarchies. The findings indicate that the Mohr–Coulomb envelope model does not adequately capture the behavior of masonry shear. This highlights the necessity for data-driven modeling strategies that are tailored to specific interfaces..

Keywords: *Masonry Shear Behavior; Triplet Shear Test; Mortar–Brick Interface; Cohesion And Friction; Data-Driven Analysis.*

*** Correspondence Author**

Cite This Article: Abdelkader, Y. O., Wardeh, G., Fares, H., & Al-Mahmoud, F. (n.d.). Interface-Controlled Shear Behavior of Masonry: Insights from a Database of Triplet Tests. *Steps For Civil, Constructions and Environmental Engineering*, *4*(2), 14–24. https://doi.org/10.61706/sccee12011272

Introduction

The shear behavior of masonry is a governing factor in the structural performance of masonry systems, particularly under lateral actions such as seismic and wind loads. Due to its composite nature, comprising masonry units, mortar, and their interface, masonry exhibits inherently heterogeneous and nonlinear behavior. The failure mechanisms of these materials are primarily governed by the response of bed joints and interfaces, where sliding, cracking, or combined modes of failure may develop. Consequently, an accurate and reliable characterization of shear properties is imperative for structural assessment and modeling (NF EN 1052-3, 2003).

The triplet shear test has emerged as the reference experimental method for characterizing the shear response of masonry bed joints under controlled conditions. The application of a constant normal compressive load in conjunction with shear loading reproduces representative stress states, thereby enabling the direct identification of key parameters, namely cohesion and friction angle. These parameters are commonly interpreted within the framework of the Mohr–Coulomb failure criterion (Andreotti et al., 2018; Monteferrante et al., 2025; NF EN 1052-3, 2003) and form the backbone of most analytical and numerical models of masonry behavior (Bompa & Elghazouli, 2020; Dhir et al., 2022).

Nevertheless, despite the extensive experimental research conducted over the course of several decades, the behavior of masonry shear remains challenging to predict with any degree of reliability. A review of the extant literature reveals substantial scatter in experimental results, even for nominally similar materials. This variability is not incidental but rather is indicative of the substantial influence of numerous interacting factors, including unit strength, mortar composition, interface roughness, and workmanship quality (Collin et al., 2025, 2026; Magagnini et al., 2025; Milani et al., 2014). A significant problem in the existing literature pertains to the incomplete reporting of experiments, which often includes missing mechanical properties or partially defined failure parameters. This lack of consistency severely limits the comparability of findings across studies and undermines the robustness of existing models.

Consequently, contemporary modeling practices frequently entail the utilization of oversimplified assumptions, most notably the adoption of a single linear Mohr–Coulomb envelope to represent a broad spectrum of masonry systems. Such approaches are fundamentally inadequate, as they neglect the material-specific and interface-driven nature of shear behavior. This finding unveils a conspicuous and unresolved research gap: the dearth of a robust, data-driven framework capable of capturing the variability of masonry shear response and identifying its governing parameters.

In response, the present study has developed a comprehensive, literature-based database of masonry triplet shear tests and performed a systematic and quantitative analysis of the relationships between material properties and shear parameters. The methodology under consideration combines statistical correlation analysis with simple yet interpretable predictive techniques, including regression and nearest-neighbor approaches. These techniques are specifically suited to small and heterogeneous datasets. By leveraging a substantial and varied array of experimental results, the study critically evaluates the extent to which commonly reported mechanical properties can explain or predict shear behavior.

The contributions of this work are threefold and directly address the identified limitations in the literature: The construction and harmonization of an extensive experimental database is necessary to enable consistent cross-study analysis. The demonstration that compressive strength parameters alone are insufficient to explain shear behavior is essential, as it highlights the dominant role of interface-related factors. The validation of simple, data-driven predictive strategies capable of capturing global trends while preserving physical interpretability is also crucial.

Principle of Triplet Test

The triplet test is a standardized method used to characterize the shear behavior of masonry bed joints. This test involves isolating the response of the mortar and the brick–mortar interface under controlled conditions (NF EN 1052-3, 2003). The specimen under consideration consists of three masonry units that have been bonded by two horizontal mortar joints, forming a small representative segment of a wall (see Figure 1). During the test, a constant vertical compressive load is used to simulate the overburden stresses present in real structures. A horizontal shear force is applied to the central unit to induce sliding along the two joints. This configuration produces an approximately uniform shear stress state, allowing for the evaluation of the mechanical properties of the joints.

The calculation of the average shear stress is derived from the principle of simultaneous activation of two joints, which results in the expression $\tau = \frac{F}{2A}$, where F signifies the applied shear force and A represents the area of one joint. By varying the standard compression, key parameters such as cohesion and friction angle can be determined, typically using the Mohr–Coulomb failure criterion. Consequently, the triplet test is a foundational instrument for comprehending masonry behavior and for calibrating analytical and numerical models.

The triplet shear test provides direct measurements of the shear response of masonry bed joints under different levels of applied normal compression. The test, as demonstrated by the force–displacement curves, has the capacity to determine several key parameters. These include the initial shear stiffness, the peak shear strength, and the post-peak behavior. The post-peak behavior is associated with sliding or cracking along the joints. A series of experiments were conducted to ascertain the relationship between shear strength and applied normal stress. The experiments involved varying the vertical compressive load, thereby generating a data set from which a clear relationship could be determined. This relationship is commonly interpreted through the Mohr–Coulomb failure criterion, which states that the shear strength increases linearly with normal compression according to the following equation:

$$\tau = c + \sigma_n \tan\phi \qquad (1)$$

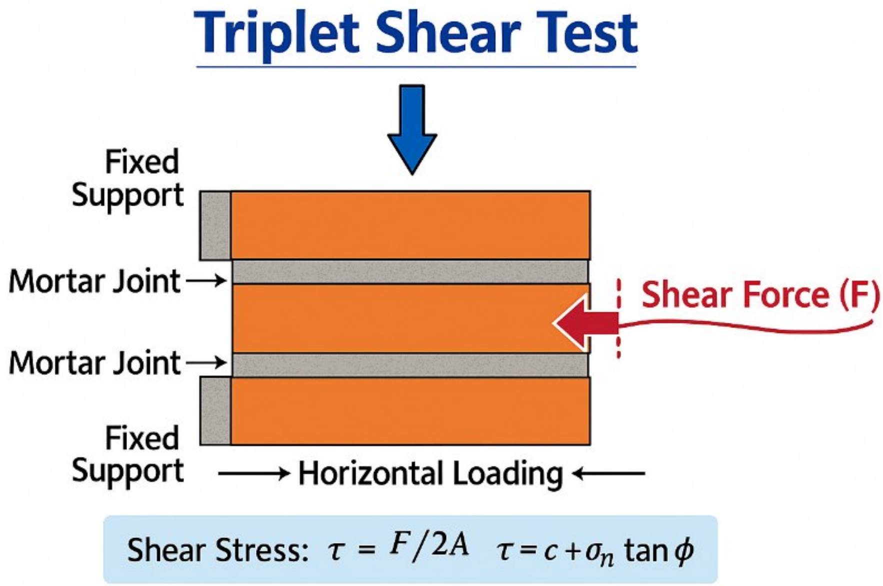

Figure 1. Configuration of the Triplet Shear Test Used to Measure Masonry Shear Strength.

The analysis of the peak shear stress values in relation to the corresponding normal stresses facilitates the extraction of two fundamental parameters that govern joint behavior: cohesion (c), which represents the shear resistance at zero normal load, and the friction angle (φ), which expresses the rate at which shear strength increases with increasing compression. The resulting linear envelope not only characterizes the mechanical properties of the mortar–brick interface but also provides essential input parameters for analytical models and numerical simulations of masonry structures.

Literature-Based Masonry Dataset

The dataset presented in Table 1 encompasses the mechanical and interface properties documented in a comprehensive array of experimental investigations on masonry triplet shear tests (Abdou et al., 2006; Andreotti et al., 2018; Barattucci et al., 2020; Bompa & Elghazouli, 2020; Dhir et al., 2022; Lavado & Gallardo, 2019; Magagnini et al., 2025; Pavan & Nanjunda Rao, 2016; Prakash & Alagusundaramoorthy, 2008; Rob van der Pluijm, 1999; Thomas Zimmermann & Alfred Strauss, 2011; Zimmermann et al., 2012). These studies furnish a comprehensive reference framework for the evaluation of the diversity of mortar-brick interfaces encountered across a range of materials, manufacturing techniques, and construction traditions. In the majority of cases, essential parameters, including brick compressive strength, mortar mix proportions, mortar compressive strength, and interface behavior indices (cohesion and friction angle), were available and could be incorporated directly into the comparative analysis performed in this study.

However, a review of several publications reveals significant gaps in experimental reporting, which limit the ability to fully normalize or compare their results on a consistent mechanistic basis. Specifically, Van der Pluijm (Rob van der Pluijm, 1999) reports interface parameters (cohesion and friction angle) but does not provide brick or mortar strength values for any of the nine tested series, thereby preventing a complete mechanical characterization of the assemblies. Similarly, Lavado and Gallardo's (Lavado & Gallardo, 2019) study omits both brick and mortar strengths for the two clay masonry series tested in Lima, thereby restricting its comparability to studies with more complete datasets. In the work of Zimmermann (Thomas Zimmermann & Alfred Strauss, 2011; Zimmermann et al., 2012), brick and mortar strengths are reported; however, cohesion values are not provided (recorded as "nan" in the original datasets). This precludes the reconstruction of the full Mohr–Coulomb envelope. Barattucci et al. (Barattucci et al., 2020) report on mortar strength and detailed interface behavior; however, they do not provide brick compressive strength for any of the three mortar series that were tested. Finally, Pavan and Nanjunda Rao (Pavan & Nanjunda Rao, 2016) and Prakash and Alagusundaramoorthy (Prakash & Alagusundaramoorthy, 2008) report most mechanical quantities but do not include the friction angle, again limiting the completeness of the Mohr–Coulomb parameters derivable from their results.

Notwithstanding the aforementioned omissions, the database under consideration constitutes a comprehensive collection of triplets-test-based findings, integrating 183 individual shear tests sourced from the extant literature and summarized in Figure 2. Each point in the figure corresponds to a single triplet specimen, where the horizontal axis denotes the applied normal stress and the vertical axis represents the measured peak shear stress at failure. The aggregated dataset displays a wide dispersion of shear-strength values across materials, mortar compositions, and manufacturing processes.

It has been demonstrated that certain datasets exhibit particularly pronounced variability. For instance, the Van der Pluijm series (Rob van der Pluijm, 1999) demonstrates the widest scatter, with shear strengths ranging from approximately 0.5 MPa to more than 2.8 MPa under normal stresses of up to 1 MPa. This phenomenon is likely a consequence of the aggregation of numerous mortar-brick combinations, which introduces material heterogeneity that cannot be resolved due to the absence of strength data. Lavado and Gallardo (Lavado & Gallardo, 2019) further emphasize the impact of the manufacturing process, noting that handmade bricks consistently exhibit lower shear strengths (0.2–0.6 MPa) compared to industrially manufactured perforated units, which reach values up to 0.7 MPa under similar normal stresses.

The Magagnini et al. (Magagnini et al., 2025) dataset displays anomalous dispersion within a restricted stress range, potentially indicative of the compromised state of the historic mortars examined or disparities between the Type□A and Type□B blends. A comprehensive analysis of the compiled dataset reveals a substantial reference base for interpreting shear behavior across a range of masonry configurations. However, the analysis also highlights a persistent issue: the incomplete documentation of experiments in the existing literature. The absence of these parameters hinders the ability to make precise cross-study comparisons and necessitates a meticulous interpretation when integrating heterogeneous datasets into unified material models or analytical frameworks. Furthermore, the pronounced scatter observed across the test results demonstrates that a single linear relationship between normal stress (σ) and shear strength (τ) is insufficient to capture the variability in masonry shear response. The observed variations in brick type, mortar composition, manufacturing quality, and interface behavior result in distinctly different σ–τ trends. This indicates that a universal Mohr–Coulomb envelope does not accurately represent masonry. Instead, these findings underscore the imperative for material-specific or class-specific shear models, as well as more systematic experimental reporting, to attain predictive accuracy.

Correlation Analysis of Parameters Influencing Masonry Shear Behavior

The correlation matrix is a tool used to quantify linear relationships between pairs of variables. The values in the correlation matrix range from −1, indicating a perfect negative correlation, to +1, indicating a perfect positive correlation. The construction of this model entails the computation of the Pearson correlation coefficient for every pair of selected variables. In this study, the selected variables are brick compressive strength (f_b), mortar compressive strength (f_j), cohesion (c), and friction coefficient ($\tan \phi$). The calculation of each coefficient is derived as the covariance of the two variables divided by the product of their standard deviations, employing the available data after the removal of rows with missing values. The resulting matrix is found to be symmetric, with diagonal terms equal to unity, and off-diagonal terms indicating the degree of correlation (Figure 3).

The obtained values reveal generally weak relationships: brick strength shows negligible correlation with both cohesion (≈ 0.05) and friction (≈ 0.11), while mortar strength exhibits only a modest correlation with the friction parameter (≈ 0.29) and a very weak one with cohesion (≈ 0.06). Additionally, the near-zero correlation between cohesion and friction (≈ −0.03) substantiates their statistical independence. These findings suggest that compressive strengths alone may not adequately explain the variability in shear behavior, indicating the probable influence of additional interface-related parameters.

Figure 4.a provides a mechanical interpretation of the dataset by plotting shear stress (τ) as a function of normal stress (σ_n) for different categories of mortar strength. A clear increasing trend is observed across all categories, consistent with the Mohr–Coulomb failure criterion, where shear resistance grows with normal stress. While higher mortar strength is often associated with higher shear stress values, particularly under larger normal stresses, the data demonstrate substantial variability within each category. This dispersion is consistent with the weak correlations identified in the

matrix, thereby confirming that mortar strength alone is insufficient for predicting shear behavior. For a given normal stress level, the significant variation in shear stress values indicates that other factors, such as bond quality, surface roughness, and workmanship, are also contributing elements.

Table 1. Dataset of Brick and Mortar Strength Parameters from Experimental Studies.

Reference	**Series ID**	**Unit Type**	**Mortar Type**	**Mortar Mix**	**f_b (MPa)**	**f_j (MPa)**	**c (MPa)**	**tanϕ**
Van Der Pluijm (Rob van der Pluijm, 1999)	wc-J090 + 1:2:9	Clay brick (wire-cut)	GPM	1:2:9			0.88	1.01
	wc-J090 + 1:1/2:4 1/2	Clay brick (wire-cut)	GPM	1:1/2:4 1/2			0.73	0.82
	sm-VE + 1:2:9	Soft-mud brick VE	GPM	1:2:9			0.68	0.81
	sm-VE + 1:1/2:4 1/2	Soft-mud brick VE	GPM	1:1/2:4 1/2			1.15	0.98
	wc-J096 + 1:1:6	Clay brick (wire-cut)	GPM	1:1:6			0.96	0.87
	CS-brick90 + 1:2:9	Calcium silicate brick	GPM	1:2:9			0.14	0.73
	CS-brick90 + 1:1/2:4 1/2	Calcium silicate brick	GPM	1:1/2:4 1/2			0.28	0.79
	CS-block96 + TLM	Calcium silicate block	TLM	thin layer			1.1	0.61
	hswc-J0K + TLM	High-strength wire-cut brick	TLM	thin layer			4.76	1.17
Lavado and Gallardo (Lavado & Gallardo, 2019)	Lima-IND (industrial)	Industrial clay bricks (holes)	Cement-sand (no lime)	1:3 & 1:5			0.288	0.26
	Lima-ART (handmade)	Handmade clay bricks (frogs)	Cement-sand (no lime)	1:3 & 1:5			0.2364	0.25
Zimmermann (Thomas Zimmermann & Alfred Strauss, 2011; Zimmermann et al., 2012)	Group A (mix II)	Old solid brick (Vienna, 19th c.)	Lime–cement mortar	Mixture II	19.28	3.58		0.21
	Group B (mix IV)	Old solid brick (Vienna, 19th c.)	Lime mortar (very weak)	Mixture IV	19.28	0.22		0.027
Bompa and Elghazouli (Bompa & Elghazouli, 2020)	TD	Clay brick	NHL5 lime mortar	1:3	9.0	1.29	0.165	0.619
Magagnini (Magagnini et al., 2025)	T	Historic clay brick	Type A	1:1:5	27.65	3.42	0.15	0.76
	R	Historic clay brick	Type B	1:3	27.65	0.48	0.13	0.21
Pavan and Nanjunda Rao (Pavan & Nanjunda Rao, 2016)	Co	Solid burnt clay brick	Cement-sand mortar	1:6	7.65	7.0	0.33	
Andreotti et al. (Andreotti et al., 2018)	CS	Calcium silicate brick	Cement mortar		18.67	7.24	0.12	0.42
Barattucci et al.(Barattucci et al., 2020)	1:3	Fired clay brick	MC	1:3		15.57	0.932	46.1
	1:6	Fired clay brick	MC	1:6		6.06	0.796	45.5
	1:9	Fired clay brick	MC	1:9		2.04	0.356	43.0
Dhir et al. (Dhir et al., 2022)	Mortar	Fired clay brick	Ready-mix mortar	1:3–1:4	15.37	16.47	0.6	1.04
Prakash and Alagusundaramoorthy (Prakash & Alagusundaramoorthy, 2008)	STS	Low-stiffness clay brick	Cement mortar	1:5	9.6	7.1		
Abdou et al. (Abdou et al., 2006)	Solid brick	Solid clay brick	Bat Express	Ready to use	41.99	20.0	1.61	1.05

GPM = General Purpose Mortar; TLM = Thin Layer Mortar; MC = Mortar Cement.

Figure 4.b provides a complementary analysis by presenting the statistical distribution of shear stress for each mortar strength class through boxplots. A gradual increase in median shear stress with increasing mortar strength can be observed, indicating a general positive influence. However, the wide interquartile ranges and the considerable overlap between categories emphasize the high variability of the data. This overlap directly reflects the low correlation coefficients observed in the matrix and demonstrates that similar shear stress values can be obtained for a wide range of mortar strengths. The combined interpretation of the correlation matrix and the two subfigures confirm that while mortar strength exerts a secondary influence, primarily on the frictional component, normal stress remains the dominant parameter. Furthermore, the shear response is strongly affected by additional interface-related factors not explicitly captured in the dataset.

The correlation matrix displayed in Figure 5 demonstrates the linear relationships between mortar binder ratios (Cement/Binder, Lime/Binder, Sand/Binder) and the two key shear strength parameters: cohesion (c) and friction angle (tan ϕ). A robust negative correlation of −1.00 is evident between Cement/Binder and Lime/Binder, suggesting an inverse relationship that is anticipated, given that these two binders are complementary components in the mortar mixture. The study found a moderate positive correlation between cement/binder and both cohesion (0.16) and tanϕ (0.47). In contrast, Lime/Binder demonstrates a weak negative correlation with both cohesion (–0.16) and tanϕ (–0.47). The most notable finding is the strong positive correlation between sand/binder and tanϕ (0.68), suggesting that higher sand content in the mortar is associated with increased friction angle. This is a physically meaningful relationship because sand particles contribute to internal friction. Conversely, Sand/Binder exhibits a negligible negative correlation with cohesion (–0.03), suggesting that sand content exerts minimal influence on cohesion. The relationship between cohesion and tanϕ is moderately positive (0.28), suggesting that materials with higher cohesion tend to exhibit slightly higher friction angles. However, the correlation is not strong. The analysis of the matrix indicates that the composition of the mortar, particularly the ratio of sand to binder, exerts a more significant influence on friction angle than on cohesion. Conversely, the proportions of cement and lime primarily affect the binder balance, with a relatively limited direct effect on shear parameters.

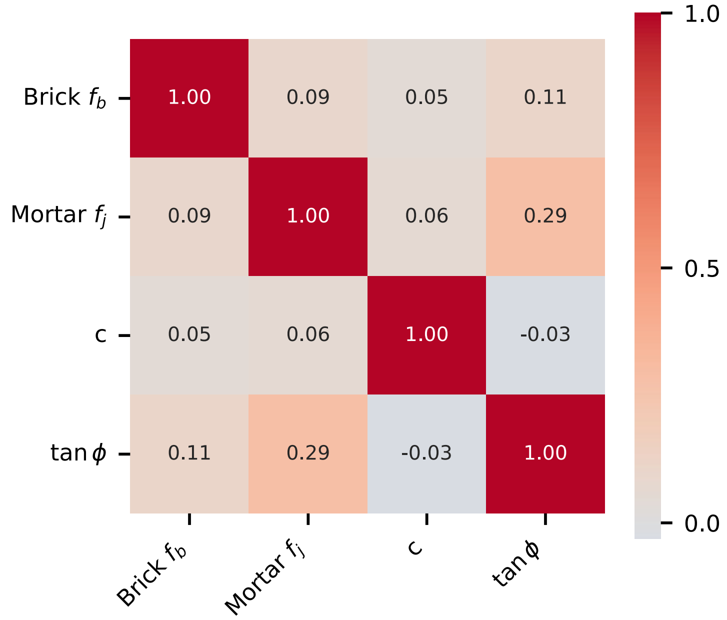

Figure 2. Correlation Matrix of Brick Strength (F_b), Mortar Strength (F_j), Cohesion (C), and Friction (Tan ϕ).

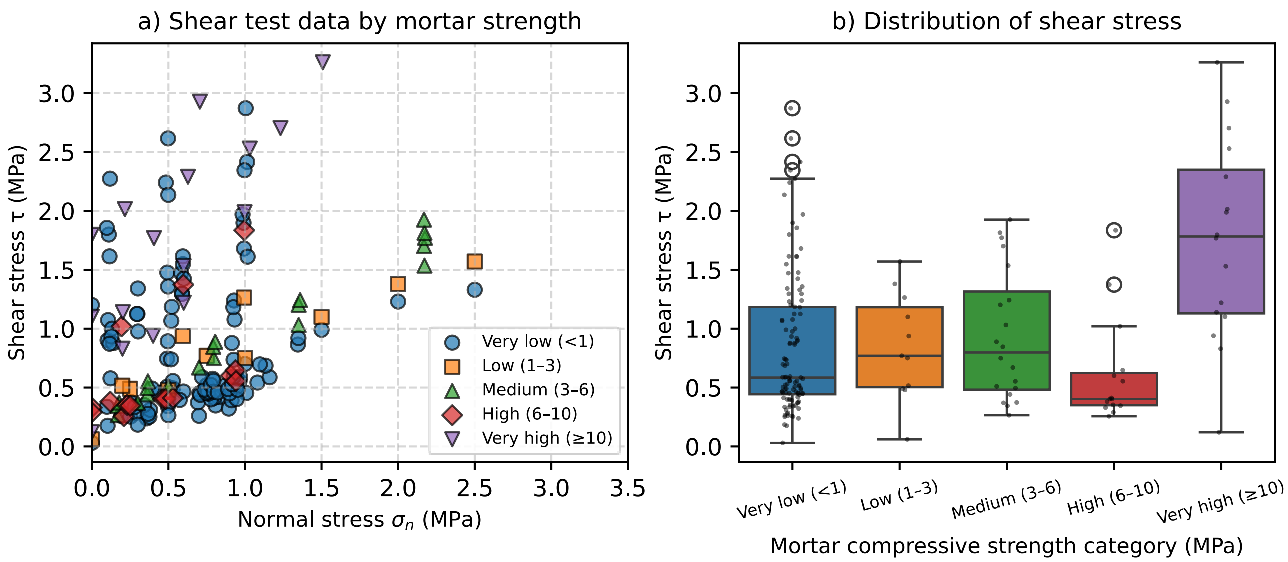

Figure 3. Shear Behavior Categorized by Mortar Strength.

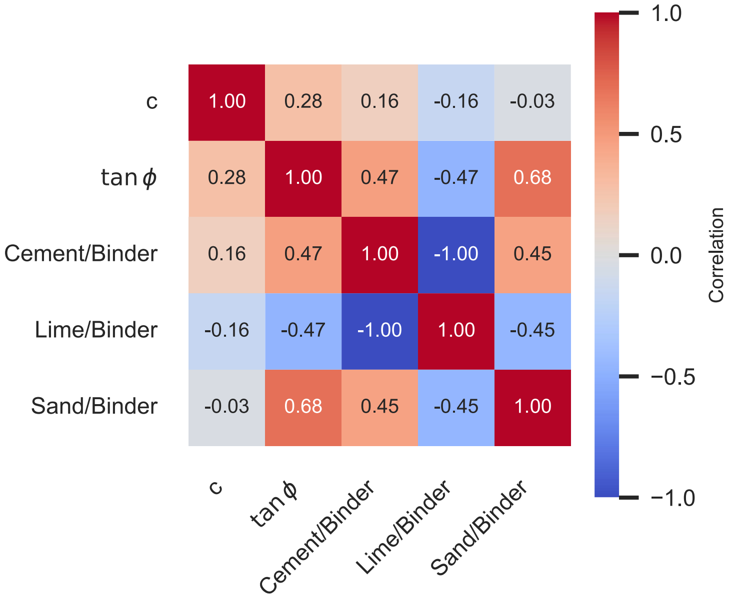

Figure 4. Correlation Matrix of Mortar Composition Parameters and Shear Parameters.

To further investigate the influence of mortar composition on shear parameters, the experimental data were grouped according to the sand-to-binder ratio into three categories (low, medium, and high) based on the distribution of the dataset. As illustrated in Figure 6, the distributions of friction and cohesion are presented.

The results of the study demonstrate a systematic increase in friction with the sand-to-binder ratio. This phenomenon can be attributed to the role of granular interlock and surface roughness, which are introduced by higher sand content. These phenomena enhance resistance to sliding at the interface. In contrast, cohesion demonstrates a lack of consistent variation across the various categories and exhibits significant variability. This finding suggests that cohesion is predominantly governed by interface bonding mechanisms rather than by mortar composition. The amalgamation of these analyses corroborates the notion that friction and cohesion are governed by disparate physical mechanisms and ought to be regarded as discrete parameters. These observations are consistent with correlation analysis and reinforce the conclusion that masonry shear behavior is predominantly interface-controlled.

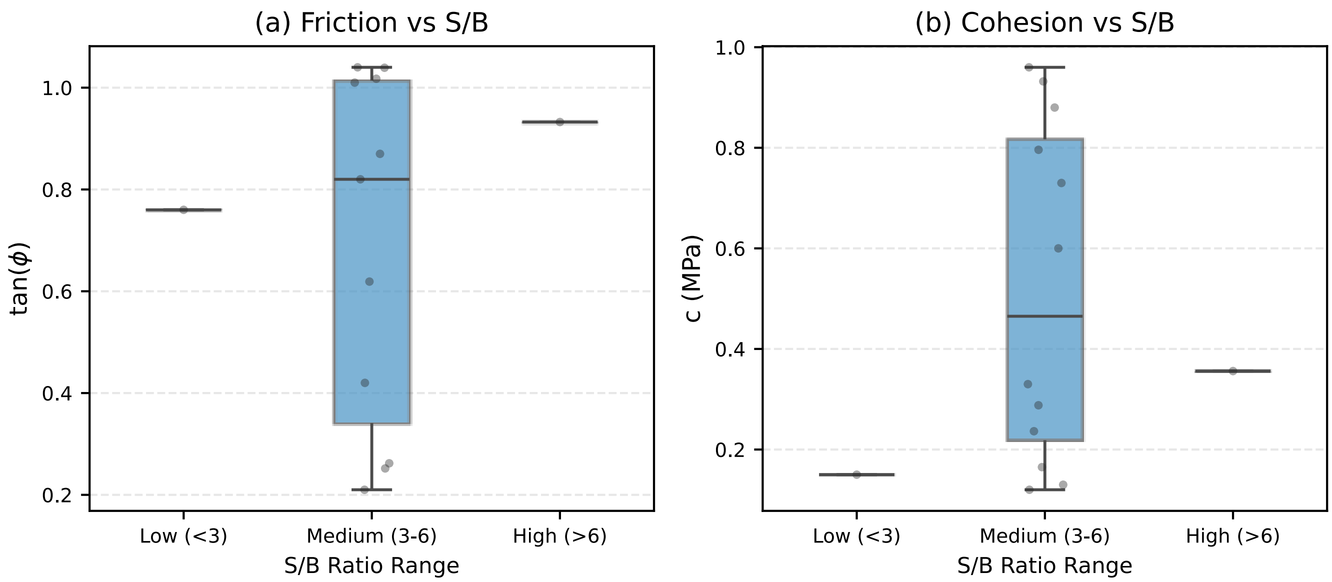

Figure 5. Friction and Cohesion Versus Sand-to-Binder Ratio.

Prediction of Masonry Shear Properties

In order to validate the robustness of the database-driven analysis presented in the previous section, a combined regression-nearest neighbor (NN) predictive strategy was benchmarked against three well-documented experimental references that span the full spectrum of masonry shear behavior. The three references are as follows: the weak aerial-lime brick masonry of Pelà et al. (2017), the normal-strength cement-sand masonry characterized by Shabdin et al. (2018) through modified triplet shear tests, and the strong limestone masonry with commercial mortar studied by Turath Gharib (2015). For each case, the mechanical properties of units and mortar, including binder ratios, were encoded into the regression-based predictive model. The neural network (NN) method was then used to locate each experimental configuration within the existing material space of the database. This approach provided a localized comparison based on the most similar mixtures. In experimental settings, a discernible hierarchical sequence was observed among the three systems under consideration. This sequence ranged from Pelà's joints, which exhibited a notably weak bond strength ($c = 0.04$MPa, $\tan\phi = 0.72$), to those of Shabdin's intermediate cement–sand mortar ($c = 0.24$MPa, $\tan\phi = 0.52$), and finally to those of Gharib's highly interlocked limestone interfaces ($c = 0.3$MPa, $\tan\phi = 1.12$).

The NN approach reproduced this ordering: The neighbors of Pelà exhibited marginally elevated levels of cohesion, yet exhibited comparable friction ($c \approx 0.2 - 0.4$MPa, $\tan\phi \approx 0.7 - 1.0$). In contrast, the neighbors of Shabdin demonstrated the archetypal characteristics of cement-mortar behavior ($c \approx 0.2 - 0.45$MPa, $\tan\phi \approx 0.5 - 0.8$). Conversely, the neighbors of Gharib exhibited pronounced adhesion and substantial interlock ($c \approx 0.4 - 0.9$MPa, $\tan\phi \approx 0.8 - 1.2$). The regression model exhibited a similar trend, yielding 0.10–0.12 MPa, 0.35–0.45 MPa, and 0.55–0.65 MPa for cohesion in (Pelà et al., 2017), (Shabdin et al., 2018), and (Turath Gharib, 2015), respectively. The model also yielded 0.75–0.85, 0.60–0.75, and 0.90–1.00 for $\tan\phi$. However, the model slightly overestimated cohesion due to the underrepresentation of weak lime mortars and stone interfaces in the database. Nonetheless, the model accurately reproduced friction. When considered as a whole, the two predictive methods consistently reconstructed the mechanical progression weak lime < normal mortar < strong stone, thereby confirming the validity of the trends identified in the database. This is particularly true with regard to the role of mortar strength and binder composition in controlling friction. When tested against independent datasets covering the entire range of masonry shear performance, these trends remained valid. A comprehensive overview of the results is provided in Table 2.

A more thorough evaluation of more complex machine learning (ML) algorithms was conducted; however, these algorithms did not perform reliably due to the limited size and high variability of the available dataset. These findings confirm that regression and nearest neighbor methods are more appropriate for small experimental databases.

It is imperative to acknowledge that the regression and nearest-neighbor approaches delineated herein are conceptualized as research-oriented instruments aimed at discerning trends within the dataset. These models are not formulated as direct design equations and require further validation before practical engineering application.

Table 2. Experimental Versus Predicted Shear Parameters.

Study	Experimental *c* (MPa)	Predicted c (MPa)	Experimental $\tan\phi$	Predicted $\tan\phi$
(Pelà et al., 2017)	0.04	0.10–0.12	0.72	0.75–0.85
(Shabdin et al., 2018)	0.24	0.35–0.45	0.52	0.60–0.75
(Turath Gharib, 2015)	0.30	0.55–0.65	1.12	0.90–1.00

Failure Modes of Masonry Assemblies

The failure mode of a masonry assembly under shear loading is contingent upon the relative strengths of the units, the mortar, and the unit–mortar interface. The shear parameters cohesion (c) and friction $\tan\phi$ exert a substantial influence on the aforementioned failure mode. As demonstrated in Figure 7, when cohesion is minimal and the interface bond is fragile, the shear stress attains the Mohr–Coulomb envelope at reduced values, thereby inducing interface mortar–block failure (Figure 7.a), where sliding transpires predominantly along the interface. When cohesion increases yet remains lower than the tensile strength of the mortar, the stress path permits limited tensile stresses to develop in the joint, resulting in combined mortar-joint cracking and interface failure (Figure 7.b). In scenarios where both cohesion and friction are adequately elevated—such as mortars with robust adhesion or units with textured surfaces—the interface strengthens beyond that of the constituent units, resulting in the propagation of diagonal tensile stresses through the blocks and across the mortar joint (Figure 7.c). This phenomenon gives rise to a mixed unit–

mortar cracking pattern. In the event that the interface demonstrates substantial strength while the mortar itself exhibits the greatest weakness, shear stresses induce pure mortar joint failure (Figure 7.d). In such instances, the cracking is predominantly confined to the mortar layer. These four mechanisms delineate a continuum that is governed by the shear parameters. Low cohesion fosters sliding, moderate cohesion enables mixed-mode failure, and high friction in conjunction with strong adhesion shifts the failure towards cracking and crushing within the masonry units. This behavioral spectrum aligns with experimental observations across a range of materials and structures, including weak aerial-lime mortars, normal-strength cement mortars, and rough-surface stone masonry.

To elucidate the manifestation of the various failure mechanisms delineated above across a comprehensive array of experimental studies, Table 3 offers a synopsis of the shear properties and observed failure modes documented in the extant literature. These properties and modes are then classified according to the four mechanisms illustrated in Figure 7. By establishing a correlation between each experimental outcome and its corresponding cohesion (c) and friction tan ϕ parameters, the table underscores the significance of interface bonding, mortar strength, and unit roughness in dictating the transition from pure sliding to mixed-mode cracking and, ultimately, to unit-controlled failure.

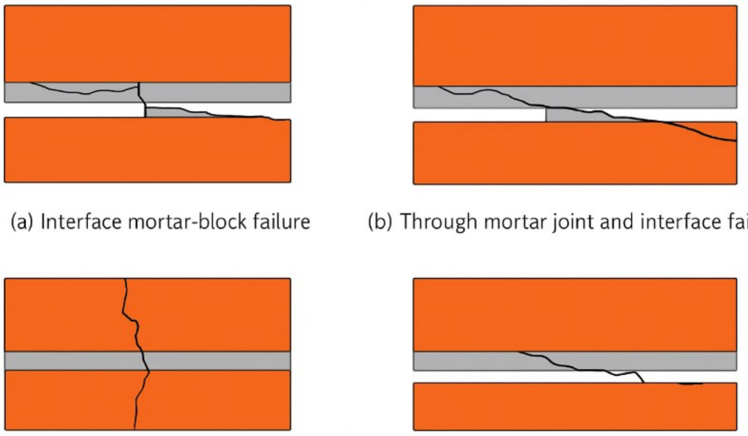

(a) Interface mortar-block failure (b) Through mortar joint and interface failure

(c) Through Jocks and mortar joint (d) Pure mortar joint failure

Figure 6. Typical Failure Modes Observed in Masonry Assemblies Under Shear Loading.

Table 3. Failure Mode Classification with Shear Interpretation.

Study	Observed Failure Mode	Classification (a–d)	Interpretation Based on Shear Properties
(Pelà et al., 2017)	Interface sliding	(a)	Very low cohesion → joint fails before any tensile resistance develops; friction insufficient to prevent sliding.
(Shabdin et al., 2018)	Mixed cracking → block cracking	(b) → (c)	Moderate cohesion allows cracking in mortar before sliding.
(Turath Gharib, 2015)	Block cracking (stone interlock)	(c)	High friction due to rough limestone surfaces → sliding prevented;
(Abdou et al., 2006)	Interface → mixed → block	(a),(b),(c)	High cohesion and high friction allow full progression of failure modes.
(Andreotti et al., 2018)	Interface decohesion	(a)	Interface behaviour dominated by sliding; friction controlled; no unit failure.
(Bompa & Elghazouli, 2020)	Sliding → mixed → block	(a)→(b)→(c)	At low cohesion: sliding; at moderate cohesion + friction: mixed failure; at high pre-compression friction increases → block cracking.

Conclusion

This study presented a data-driven investigation of masonry shear behavior based on a harmonized database of 183 triplet shear tests collected from the literature. The objective of the present study was to utilize statistical analysis and predictive benchmarking to elucidate the extent to which commonly reported mechanical properties can explain the shear parameters governing masonry joint response.

The correlation analyses demonstrate that brick and mortar compressive strengths exhibit weak or negligible relationships with cohesion and friction. This confirms that compressive strength alone is an inadequate predictor of masonry shear behavior. The influence of mortar strength on strength is secondary, affecting primarily the frictional component. In contrast, cohesion is predominantly influenced by interface quality and bond characteristics. The observed correlation between cohesion and friction underscores the multi-mechanism nature of masonry shear resistance. In contrast, the composition of mortar, particularly the proportion of sand to binder, has been identified as a pivotal parameter that exerts a significant influence on friction. This observation is indicative of the critical role that surface roughness and granular interlock play at the interface. These findings underscore the notion that masonry shear behavior is predominantly governed by interface-related properties rather than by global material strengths.

The predictive assessment, which is based on regression and Nearest-Neighbor approaches, confirms that simple, interpretable data-driven methods are well suited to small and heterogeneous experimental databases. When evaluated in comparison to independent experimental studies encompassing weak lime mortars, conventional cement mortars, and strong stone masonry, the proposed framework effectively replicates the accurate hierarchy and overall trends in shear behavior. The investigation revealed that more complex machine-learning models were found to be unreliable due to data sparsity.

Finally, the correlation of shear parameters to observed failure modes provides a unified mechanical interpretation of masonry behavior, ranging from interface sliding at low cohesion to unit-controlled cracking at high friction and adhesion. The findings indicate that the Mohr–Coulomb envelope model does not adequately represent masonry structures. This underscores the necessity for material- or class-specific shear descriptions that incorporate interface characteristics to ensure reliable modeling and assessment.

The scope of this work is constrained to monotonic loading, excluding consideration of cyclic, long-term, or creep effects. The database integrates heterogeneous sources employing a variety of methodologies, thereby introducing uncertainty. In addition, the proposed interpretations necessitate further validation prior to implementation in structural or seismic design contexts.

Declarations

Authors' Contributions

Y.O.A: Methodology, Formal analysis, Investigation, Writing of the original draft, Writing – review & editing, Visualization.

G.W: Conceptualization, Validation, Writing – review & editing, Visualization, Supervision.

H.F: Validation, Writing – review & editing, Supervision.

F.A: Validation, Writing – review & editing, Supervision.

Conflict of Interest

The authors declare that they have no known competing financial interests or personal relationships that could have appeared to influence the work reported in this paper.

Funding

This research did not receive any specific grant from funding agencies in the public, commercial, or not-for-profit sectors.

Declaration on the Use of Generative AI and AI-Assisted Technologies

The authors declare that generative artificial intelligence was used for language assistance and to improve the writing of the manuscript. The authors reviewed and edited the generated content as necessary and take full responsibility for the content of the publication.

Data Availability

The data that support the findings of this study are available from the corresponding author upon reasonable request.

Acknowledgement

The authors declare that there is no acknowledgement to be made.

Ethics

This study did not involve human participants or animals; hence, no ethical approval was required.

References

Abdou, L., Saada, R. A., Meftah, F., & Mebarki, A. (2006). Experimental investigations of the joint-mortar behaviour. *Mechanics Research Communications*, *33*(3), 370–384. https://doi.org/10.1016/j.mechrescom.2005.02.026

Andreotti, G., Graziotti, F., & Magenes, G. (2018). Detailed micro-modelling of the direct shear tests of brick masonry specimens: The role of dilatancy. *Engineering Structures*, *168*, 929–949. https://doi.org/10.1016/j.engstruct.2018.05.019

Barattucci, S., Sarhosis, V., Bruno, A. W., D'Altri, A. M., de Miranda, S., & Castellazzi, G. (2020). An experimental and numerical study on masonry triplets subjected to monotonic and cyclic shear loadings. *Construction and Building Materials*, *254*, 119313. https://doi.org/10.1016/j.conbuildmat.2020.119313

Bompa, D. V., & Elghazouli, A. Y. (2020). Experimental and numerical assessment of the shear behaviour of lime mortar clay brick masonry triplets. *Construction and Building Materials*, *262*, 120571. https://doi.org/10.1016/j.conbuildmat.2020.120571

Collin, L., Gatuingt, F., Giry, C., & Hild, F. (2025). Exploring the shear behavior of masonry triplets via digital image correlation, damage quantification and Mohr-Coulomb criterion identification. *Structures*, *80*, 109696. https://doi.org/10.1016/j.istruc.2025.109696

Collin, L., Gatuingt, F., Giry, C., & Hild, F. (2026). Identification of non linear parameters from masonry triplet shear tests using digital image correlation. *Materials and Structures*, *59*(4), 193. https://doi.org/10.1617/s11527-026-03052-1

Dhir, P. K., Tubaldi, E., Orfeo, A., & Ahmadi, H. (2022). Cyclic shear behaviour of masonry triplets with rubber joints. *Construction and Building Materials*, *351*, 128356. https://doi.org/10.1016/j.conbuildmat.2022.128356

Lavado, L., & Gallardo, J. (2019). Shear strength of brick mortar interface for masonry in Lima city. *TECNIA*, *29*(2). https://doi.org/10.21754/tecnia.v29i2.707

Magagnini, E., Nicoletti, V., & Gara, F. (2025). Experimental and Numerical Investigation of Historic Brickwork Masonry with Weak and Degraded Joints: Failure Mechanisms Under Compression and Shear. *Buildings*, *15*(21), 3993. https://doi.org/10.3390/buildings15213993

Milani, G., Simoni, M., & Tralli, A. (2014). Advanced numerical models for the analysis of masonry cross vaults: A case-study in Italy. *Engineering Structures*, *76*, 339–358. https://doi.org/10.1016/j.engstruct.2014.07.018

Monteferrante, C., Ferretti, F., & Savoia, M. (2025). Large-scale seismic vulnerability assessment of masonry buildings through a simplified methodology. *Bulletin of Earthquake Engineering*. https://doi.org/10.1007/s10518-025-02319-2

NF EN 1052-3. (2003). *Methods of test for masonry - Part 3 : determination of initial shear strength*.

Pavan, G. S., & Nanjunda Rao, K. S. (2016). Behavior of Brick–Mortar Interfaces in FRP-Strengthened Masonry Assemblages under Normal Loading and Shear Loading. *Journal of Materials in Civil Engineering*, *28*(2). https://doi.org/10.1061/(ASCE)MT.1943-5533.0001388

Pelà, L., Kasioumi, K., & Roca, P. (2017). Experimental evaluation of the shear strength of aerial lime mortar brickwork by standard tests on triplets and non-standard tests on core samples. *Engineering Structures*, *136*, 441–453. https://doi.org/10.1016/j.engstruct.2017.01.028

Prakash, S. S., & Alagusundaramoorthy, P. (2008). Load resistance of masonry wallettes and shear triplets retrofitted with GFRP composites. *Cement and Concrete Composites*, *30*(8), 745–761. https://doi.org/10.1016/j.cemconcomp.2007.11.005

Rob van der Pluijm. (1999). *Out-of-plane bending of masonry behaviour and strength*. Technische Universiteit Eindhoven.

Shabdin, M., Zargaran, M., & Attari, N. K. A. (2018). Experimental diagonal tension (shear) test of Un-Reinforced Masonry (URM) walls strengthened with textile reinforced mortar (TRM). *Construction and Building Materials*, *164*, 704–715. https://doi.org/10.1016/j.conbuildmat.2017.12.234

Thomas Zimmermann, & Alfred Strauss. (2011). Variation of shear strength of masonry with different mortar properties. *The North American Masonry Conference (NAMC)*, 1–14.

Turath Gharib. (2015). *Strengthening of Historical Masonry Structures with Composite Materials: Application to Limestone Walls* [Ph.D thesis]. Université Claude Bernard Lyon 1 (University of Lyon 1), France.

Zimmermann, T., Strauss, A., & Bergmeister, K. (2012). Structural behavior of low- and normal-strength interface mortar of masonry. *Materials and Structures*, *45*(6), 829–839. https://doi.org/10.1617/s11527-011-9801-2